The Meteoritical Society

Meteoritics & Planetary Science 1–15 (2015)
doi: 10.1111/maps.12506

Screening and classification of ordinary chondrites by Raman spectroscopy

Lidia PITTARELLO[1*], Kitty BAERT[2], Vinciane DEBAILLE[3], and Philippe CLAEYS[1]

[1]Earth System Science, Analytical, Environmental and Geo-Chemistry (AMGC), Vrije Universiteit Brussel, Pleinlaan 2, 1050 Brussels, Belgium
[2]Materials and Chemistry, Research Group Electrochemical and Surface Engineering (SURF), Vrije Universiteit Brussel, Pleinlaan 2, 1050 Brussels, Belgium
[3]Laboratoire G-Time, Geochemistry: Tracing with isotopes, minerals and elements, Université Libre de Bruxelles, Av. F.D. Roosevelt 50, 1050 Brussels, Belgium
[*]Corresponding author. E-mail: lidia.pittarello@vub.ac.be

(Received 19 May 2014; revision accepted 12 July 2015)

Abstract–Classification of ordinary chondrite meteorites generally implies (1) determining the chemical group by the composition in endmembers of olivine and pyroxene, and (2) identifying the petrologic group by microstructural features. The composition of olivine and pyroxene is commonly obtained by microprobe analyses or oil immersion of mineral separates. We propose Raman spectroscopy as an alternative technique to determine the endmember content of olivine and pyroxene in ordinary chondrites, by using the link between the wavelength shift of selected characteristic peaks in the spectra of olivine and pyroxene and the Mg/Fe ratio in these phases. The existing correlation curve has been recalculated from the Raman spectrum of reference minerals of known composition and further refined for the range of chondritic compositions. Although the technique is not as accurate as the microprobe for determining the composition of olivine and pyroxene, for most of the samples the chemical group can be easily determined by Raman spectroscopy. Blind tests with ordinary chondrites of different provenance, weathering, and shock stages have confirmed the potential of the method. Therefore, we suggest that a preliminary screening and the classification of most of the equilibrated ordinary chondrites can be carried out using an optical microscope equipped with a Raman spectrometer.

INTRODUCTION

Ordinary chondrites are the most common meteorites in the world (Weisberg et al. 2003). Since 2009, joint Belgian–Japanese expeditions in Antarctica have brought back hundreds of new meteorites. New meteorites must be classified for the submission and the approval of their name, as well as for meteorites collected in Antarctica by other missions (e.g., ANSMET) and for those found in the Sahara area (e.g., Idomar et al. 2014). Ordinary chondrites dominate in the historical collections in museums (e.g., Krot et al. 2005) and among the newly collected meteorites. Classification of ordinary chondrites is time consuming and requires qualified scientists. The classification of the Belgian–Japanese ordinary chondrites is done at the National Institute of Polar Research (NIPR) through two analytical steps (1) evaluation of the Fa and Fs content in olivine and in low-Ca pyroxene, respectively, for determining the chemical group by electron microscopy and (2) identification of the petrologic group (from 3 to 6, depending on the metamorphic grade), weathering, and possibly shock stage by optical microscopy (e.g., Weisberg et al. [2003] and references therein). The Fe range for chemical group is generally expressed as endmember content. For olivine, the endmembers are fayalite (Fa), with formula Fe_2SiO_4, and forsterite (Fo), with mineral formula Mg_2SiO_4. For low-Ca pyroxene, the endmembers are enstatite (En), with mineral formula $Mg_2Si_2O_6$, and ferrosilite (Fs), with mineral formula $Fe_2Si_2O_6$. The chemical groups in ordinary chondrites are: H ($Fa_{16–20}$ and $Fs_{14–18}$), L ($Fa_{22–26}$ and $Fs_{19–22}$), and LL ($Fa_{27–32}$ and $Fs_{22–26}$), according to the definition in Van Schmus and Wood

© The Meteoritical Society, 2015.

(1967) and in Hutchison (2004). The chemical analyses are generally performed with electron microprobe (EMPA) at the NIPR or quantitative energy-dispersive X-ray spectroscopy (EDX) coupled to a scanning electron microscope (SEM) at the Royal Belgian Institute of Natural Science, where a part of the collection is stored (e.g., Yamaguchi et al. 2014). These analyses require mineral standards for a trustworthy calibration of the composition. The quality of the measurements depends also on the accuracy in sample preparation (especially the polishing of the surface, which can strongly affect the measurements, but also the thickness of the carbon coating) and on the quality of operation conditions (high vacuum). These instruments may not be present in all institutes where meteorites are curated, and require a skilled operator. These factors negatively affect the possibility to have large historical or newly acquired collections being quickly classified or checked. Other classification techniques, such as oil immersion (Lunning et al. 2012) are used in other institutions for the chemical classification of ordinary chondrites from Antarctica, but also in this case skilled operators and sample preparation (a rough mineral separation) are required. A nondestructive alternative was proposed by Rochette et al. (2003), using magnetic susceptibility. Although having produced convincing results, this method can be sensitive to the heterogeneous metal distribution in the sample and to the intensity of weathering. In addition, there is a slightly different response in magnetic susceptibility between falls and finds, whereas Antarctic samples show a mixed behavior. Other techniques for the identification of the chemical group in ordinary chondrites include the bulk chemistry (Wasson and Kallemeyn 1988; Jarosewich 1990), the amount of Co in kamacite (Rubin 1990), and the abundance of siderophile elements in the bulk rock (Kallemeyn et al. 1989). Most of these last techniques imply destructive analyses (except Rubin's method), require skilled operators, and are quite time consuming.

Raman spectroscopy has already been used for meteorite characterization, but mostly for instrument calibration that will allow in situ analyses of lunar and Martian rocks (e.g., Haskin et al. [1997] and Wang et al. [2004]). The correlation between composition of olivine and pyroxene has been determined (Wang et al. 2004) and detailed work on Raman calibration for the Mg/Fe ratio in pyroxene (Huang et al. 2000; Wang et al. 2001) and in olivine (e.g., Kuebler et al. 2006) has been carried out. The potential of Raman spectroscopy has been largely exploited for the identification of shock-induced features or shock-induced polymorphs in meteorites (e.g., Wang and Chen 2006; Gillet et al. 2007). Recently, Raman spectroscopy on the structure of carbonaceous matter has allowed the detailed classification of the metamorphic stage (petrologic type) in low-grade chondrites (Bonal et al. 2006, 2014; Quirico et al. 2009). The works on Raman spectroscopy on planetary materials are uncountable and cannot all be listed here, but so far this technique has not regularly been used as a method for meteorite chemical classification.

The theory behind Raman spectroscopy can be simplified as the inelastic response of chemical bonds to the excitement induced by photons. This excitement produces a scattering of the incident light with a typical wavelength that provides information on the mineral structure, composition, and vibrational as well as the electronic states of the investigated material (e.g., Wolverson 1995). The distribution of Fe and Mg in olivine and pyroxene structures is reflected by the peak position in the Raman spectra because of the different size of the two ions, therefore providing a correlation between the obtained spectrum and the chemical composition of the analyzed grain.

Here, we propose to apply Raman spectroscopy for ordinary chondrite classification, in particular for the chemical group determination. A simplified calibration method is proposed in the range of olivine and pyroxene compositions characteristic for ordinary chondrites and the results of blind tests of classification are shown to support the potential of the technique.

SAMPLE DESCRIPTION AND ANALYTICAL METHODS

Raman spectra from reference minerals are available in the online RRUFF database (Downs 2006), and spectra were obtained from selected meteorites for the purpose of this study. The first provide a reference correlation between Raman spectra and chemical composition (Table 1) and the latter are used for checking and refining this correlation specifically for ordinary chondrites. The meteorites selected for refining the existing calibration include two type 3 ordinary chondrites and one enstatite chondrite, as following:

1. Asuka (A) 09178, an LL3 ordinary chondrite (Yamaguchi et al. 2014) collected in Antarctica in 2009 by a Belgian–Japanese joint mission (Fig. 1a).
2. Yamato (Y) 793255, an L3 ordinary chondrite, collected in Antarctica in 1979 by a Japanese mission (Fig. 1b).
3. Sahara 97079, an EH3 chondrite, paired with Sahara 97096, found in North Africa in 1997 (Fig. 1c).

Type 3 ordinary chondrites were preferentially chosen because they provide the widest range of olivine and pyroxene composition between chondrules. The

Table 1. Raman shift of selected peaks for reference minerals (peaks detected with the script *peakdet* from raw data provided by the online database RRUFF).

	Sample name	Composition	Peak A (cm^{-1})	Peak B (cm^{-1})	Peak C (cm^{-1})
Olivine	Fa R100103	Fa_{96}	814.6	836.8	–
	Fa R100102	Fa_{55}	818.0	846.0	–
	Fo R060539	Fa_{17}	822.0	853.4	–
	Fo R040057	Fa_{16}	822.0	853.4	–
	Fo R040018	Fa_{9}	822.9	854.7	–
	Fo R050117	Fa_{9}	823.5	855.3	–
	Fo R060535	Fa_{9}	823.5	855.8	–
	Fo R060551	Fa_{9}	823.5	855.3	–
	Fo R100101	Fa_{9}	823.8	855.6	–
	Fo R100100	Fa_{8}	823.8	855.6	–
	Fo R100099	Fa_{0}	825.2	857.5	–
	Fo R040052	Fa_{0}	824.5	856.8	–
Low-Ca pyroxene	Fs R070386	Fs_{84}	312.2	660.2	990.5
	Fs R070387	Fs_{52}	327.6	669.9	995.8
	En R040093	Fs_{16}	338.5	680.3	1007.2
	En R040094	Fs_{16}	338.5	681.3	1010.1
	En R060744	Fs_{15}	339.0	681.7	1008.1
	En R070418	Fs_{14}	344.4	683.9	1007.1
	En R070550	Fs_{10}	341.1	683.9	1011.2
	En R070630	Fs_{7}	n.d.	686.6	1011.5
	ClinoenR070276	Fs_{0} (clino)	341.5	687.7	1012.2
	En R070641	Fs_{0} (ortho)	343.4	685.2	1011.1

enstatite chondrite was selected for pyroxene endmember compositions. This sample contains also a few tiny (ca. 50 μm in size) grains of olivine, which has provided additional analyses for olivine endmembers. The samples were investigated in the form of polished thin sections.

For testing the method, two Raman spectroscopy instruments were used. The first is a confocal Raman microscope LabRAM HR Evolution (HORIBA Scientific), equipped with a multichannel air-cooled CCD detector (spectral resolution <1 cm^{-1}, lateral resolution 0.5 μm, axial resolution 2 μm), with a solid-state laser corresponding to green light (532 nm) and at 1.25 mW excitation with 10% filter for preventing any sample damage, available at the Vrije Universiteit Brussel (VUB). The second is a SENTERRA Dispersive Raman Microscope (BRUKER), equipped with a thermoelectrically cooled CCD (ANDOR DU420-OE) with a spectral resolution of ~9 cm^{-1} in the 100–4000 cm^{-1} range (50 × 1000 μm slit) and a continuous automatic calibration (0.1 cm^{-1} theoretical accuracy) with a solid-state laser corresponding to green light (532 nm) at 2 mW for excitation, at the Royal Belgian Institute of Natural Sciences (RBINS). In sample A 09178, pyroxene and olivine grains of six chondrules, at least three points per grain (Fig. 2) were measured with both instruments for comparison. The resulting spectra show negligible differences, with a shift in the peaks positions of less than 1 cm^{-1}. The selected chondrules were marked on a printed scan of the thin section, to analyze the exact same areas for composition.

The Raman spectra were processed with the free software package GNU Octave. The peaks were detected by means of *peakdet* MATLAB/Octave script that is a simple function of finding the maxima of a two column set of data (x and y) and returning the x value (Raman shift) corresponding to those maxima (Bilauer 2012). Maxima are determined as highest values, preceded and followed by a value lower than a certain *delta*, determined by the user. For each grain, the average Raman shift for the selected peak and the standard deviation between the point analyses were determined. The standard deviation of Raman shift in a chondrule (at least three measurements) was less than 0.06%.

The composition of olivine and pyroxene in the selected meteorites A 09178 and Y 793255 was determined with a FEI-Inspect-S scanning electron microscope (SEM), equipped with backscattered electron and EDX detectors, at the RBINS. Experimental conditions were 20 kV excitation energy, 10 mm working distance (WD), and ~5 nA beam current. The quantitative analyses are calibrated by comparison with olivine and pyroxene standards from the series MINM 25–53 from Astimex Scientific Limited. The standard deviation for olivine composition

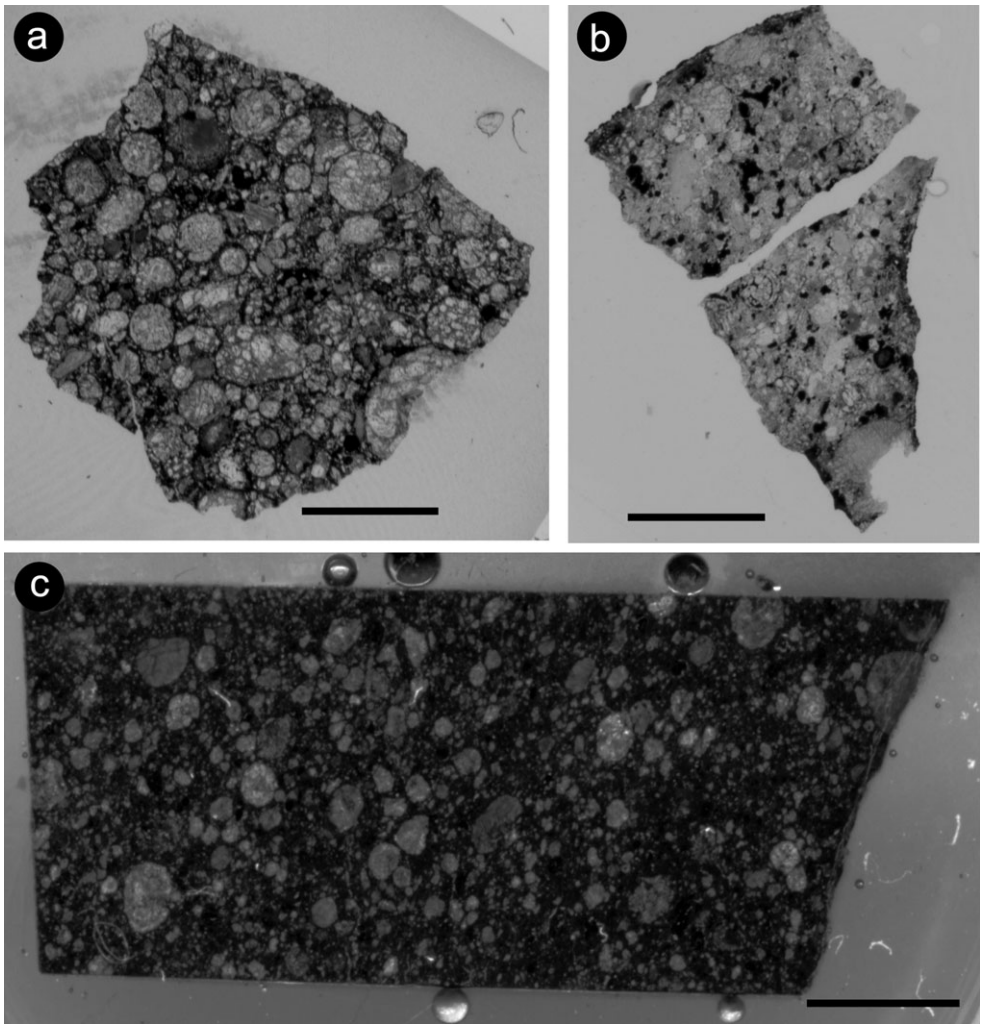

Fig. 1. Chondrite meteorites analyzed in this study. a) Sample A 09178, LL3 ordinary chondrite. b) Y 793255, L3 ordinary chondrite. c) Sahara 97079, EH3 enstatite chondrite. All pictures are thin section scans. The black bar corresponds to 3 mm.

as determined by quantitative EDX analysis on five grains per chondrule corresponds to <2%.

The composition of pyroxene and olivine, determined by microprobe analyses, from sample Sahara 97079 was provided by S. McKibbin (unpublished data) and was not checked again for this work. The chemical composition of the reference minerals, determined by microprobe, is also available in the RRUFF online database. Olivine grains with significant content of Mn (>0.5 wt%) were not considered in this study. Pyroxene samples showing significant amount of elements, other than Fe, Mg, Si, and O, were also not considered for this work. This selection is necessary because the presence of minor elements in olivine and pyroxene can have a certain influence in the Raman spectra and a calibration determined from members as pure as possible is needed as reference. The fayalite (Fa) content in olivine and the ferrosilite (Fs) content in pyroxene was estimated by mineral formula recalculation. Finally, for a linear correlation between peak position and Fa and Fs content, the MATLAB/Octave function *polyfit* was applied on the data from the reference minerals. This function computes a least squares polynomial of the chosen degree for a given set of data.

RESULTS

Calibration Curve for Olivine

The typical Raman spectrum of olivine (Figs. 2a and 3) displays two major peaks, here called Peak A, with Raman shift in the range 814–824 cm^{-1}, and Peak B, in the range 836–857 cm^{-1}. The limits of these Raman shift ranges correspond to olivine endmembers,

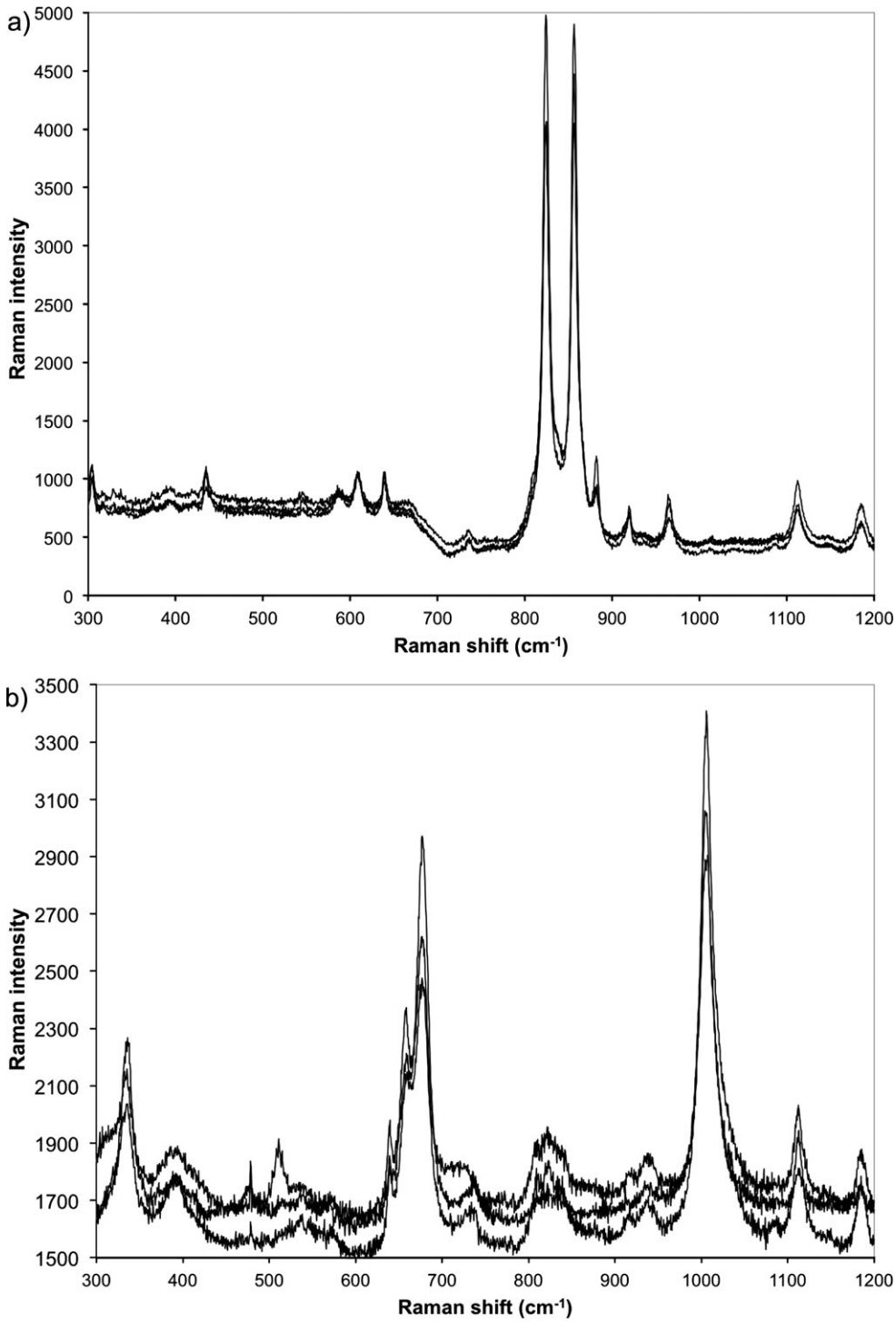

Fig. 2. Raman spectra of three grains of olivine (a) and three of pyroxene (b) from the same chondrule, respectively, in sample A 09178. Within a chondrule, the peak positions do not change.

fayalite (Fa), and forsterite (Fo) (Table 1). Intermediate compositions of olivine between the two endmembers show Raman shift of the two characteristic peaks included in the ranges given above and are defined for their Fa component mole%. Therefore, the Raman shift of Peak A and Peak B appears to have a roughly linear correlation with olivine composition (Figs. 4a and 4b). This correlation has been extrapolated from the Raman shift of Peak A and Peak B obtained from olivine grains considered as reference material, as representative

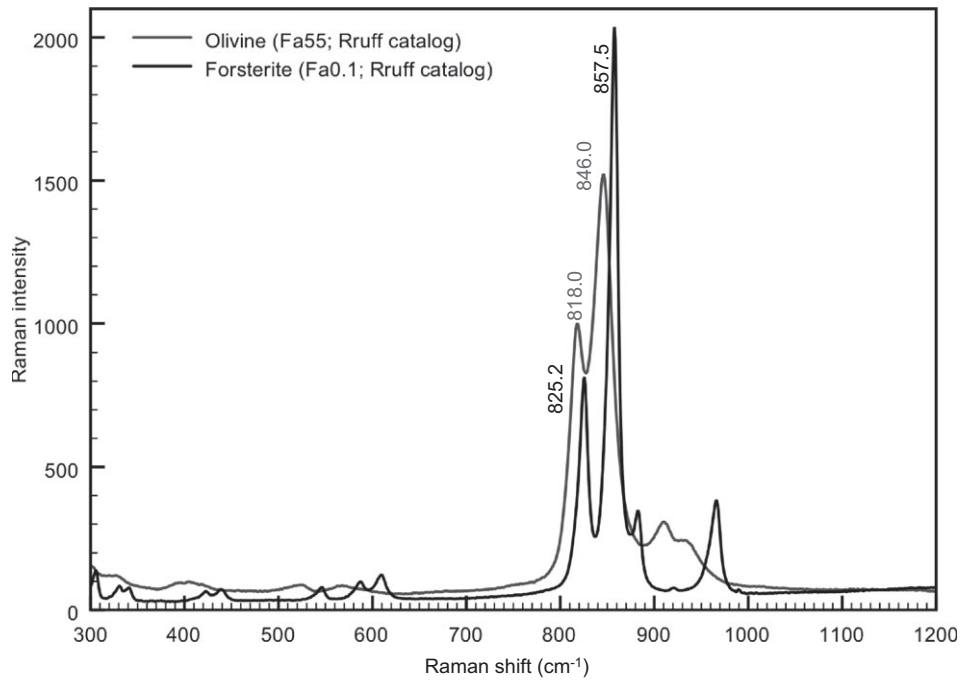

Fig. 3. Raman spectra of reference samples of olivine. Data from the online database RRUFF.

of the whole range of Fa content. The best-fit curves, giving the correlation between the Fa content and the predicted Raman shift for Peak A and Peak B, as calculated by the script *polyfit* for the reference material, are:

$$\text{Fa mole\%} = -9.13x_A + 7524 \quad (1)$$

$$\text{Fa mole\%} = -4.70x_B + 4025 \quad (2)$$

where x_A is the Raman shift corresponding to Peak A and x_B is the Raman shift corresponding to Peak B. The analyzed grains from the Antarctic meteorites have Fa content limited to 0–50 mole% (Fig. 4). In this range, the measured peak position is roughly consistent with the calculated trend. In detail, our measurements perfectly match with the correlation for Peak A (Fig. 4a), but slightly deviate from linearity for Peak B (Fig. 4b). For this reason, a different correlation between Fa content and Raman shift is proposed for Peak B, based on the limited range of our analyses on ordinary chondrites:

$$\text{Fa mole\%} = -4.55x_A + 3899.7 \quad (3)$$

Equations 1 and 3 are used for estimating the Raman shift expected for H, L, and LL chondrites (Table 2), according to the Fa values given in Hutchison (2004).

The Peak A versus Peak B diagram (Fig. 5), which shows the relative change of Raman shift with the composition (e.g., Kuebler et al. 2006), displays that the correlation is closer to a polynomial curve rather than a straight line (Fig. 5a). On the other hand, the correlation between the two peaks can be considered linear in the investigated range of data for ordinary chondrites (Fig. 5b). The deviation from a linear correlation between the Peak B position and the Fa content in olivine (Fig. 4b), does not significantly affect the peak versus peak correlation (Fig. 5b) in the considered range of composition.

Calibration Curve for Low-Ca Pyroxene

The typical Raman spectrum of low-Ca pyroxene shows three characteristic peaks, here called Peak A, with Raman shift in the range 312–341 cm^{-1}; Peak B, in the range 660–684 cm^{-1}; and Peak C, in the range 990–1011 cm^{-1} (Figs. 2b and 6; Table 1). The given range is shown by the endmembers enstatite (En) and ferrosilite (Fs). Also for low-Ca pyroxene, a correlation between the relative peak position in the Raman spectrum and the composition expressed as Fs (mole%) content does exist. The linear correlation between the Raman shift of individual peaks and the composition is more obvious for Peak B than for the other peaks (Figs. 7a–c). In the case of pyroxene, our measurements in meteorites cover a limited range of

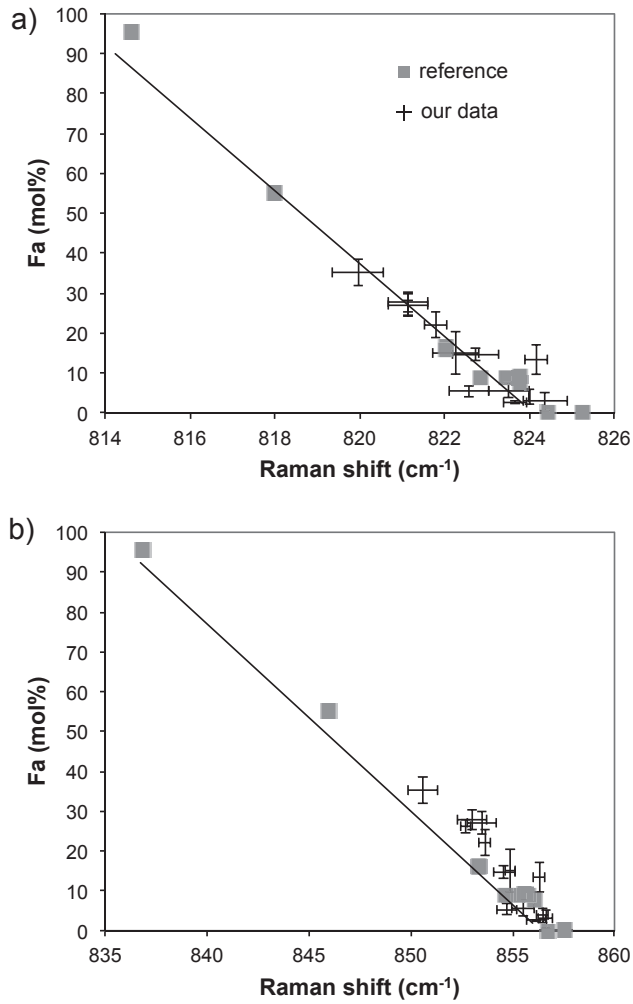

Fig. 4. Correlation between the Fa content in olivine and the Raman shift of two selected peaks (Peak A in (a) and Peak B in (b), respectively). The correlation curve has been calculated using the reference data (filled squares) and our measurements (circles) are plotted for comparison. The error bars represent the standard deviation for 3–5 Raman spectra and 3 EDS point analyses per chondrule.

composition, corresponding to $Fs_{0–20}$. Limiting the plot to this range of compositions, the correlation is not as good as it appears in the extended range (Figs. 7d–f). The uncertainty in the peak position is also increased, especially for Peak C, and in some cases the data fallout of the correlation. The best-fit curves, giving the correlation between the Fs content and the predicted Raman shift for Peak A and Peak B, as calculated by the script *polyfit* for the reference material, are:

$$\text{Fs mole\%} = -2.58x_A + 891 \quad (4)$$

$$\text{Fs mole\%} = -3.08x_B + 2116 \quad (5)$$

Table 2. Chemical group attribution based on theoretical Raman peak position, calculated from the best-fit curve for the reference spectra with *polyfit* function in MATLAB/Octave. Values for Fa and Fs content according to Hutchison (2004) and references therein and Kessel et al. (2007).

Chemical group		Peak A (cm^{-1})	Peak B (cm^{-1})	Peak C (cm^{-1})
H	$Fa_{16–20}$	821.9–822.3	852.5–853.4	–
	$Fs_{14–18}$	337.9–339.5	681.2–682.5	1007.8–1009.0
L	$Fa_{22–26}$	821.3–821.7	851.2–852.1	–
	$Fs_{19–22}$	336.5–337.6	679.9–680.8	1006.6–1007.5
LL	$Fa_{26–32}$	820.6–821.3	849.9–851.2	–
	$Fs_{22–26}$	334.9–336.5	678.6–679.9	1005.5–1006.6

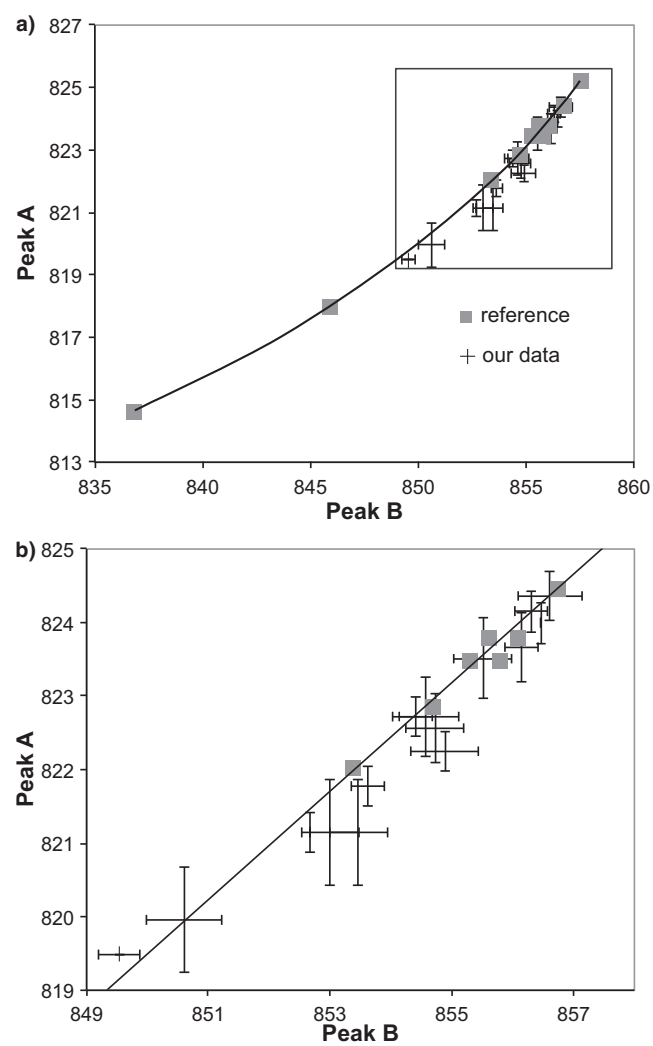

Fig. 5. Peak versus peak plot for olivine for data shown in Fig. 4. The whole peaks position range between the two endmembers is shown in (a). The range related to our measurements in meteorites is shown in (b).

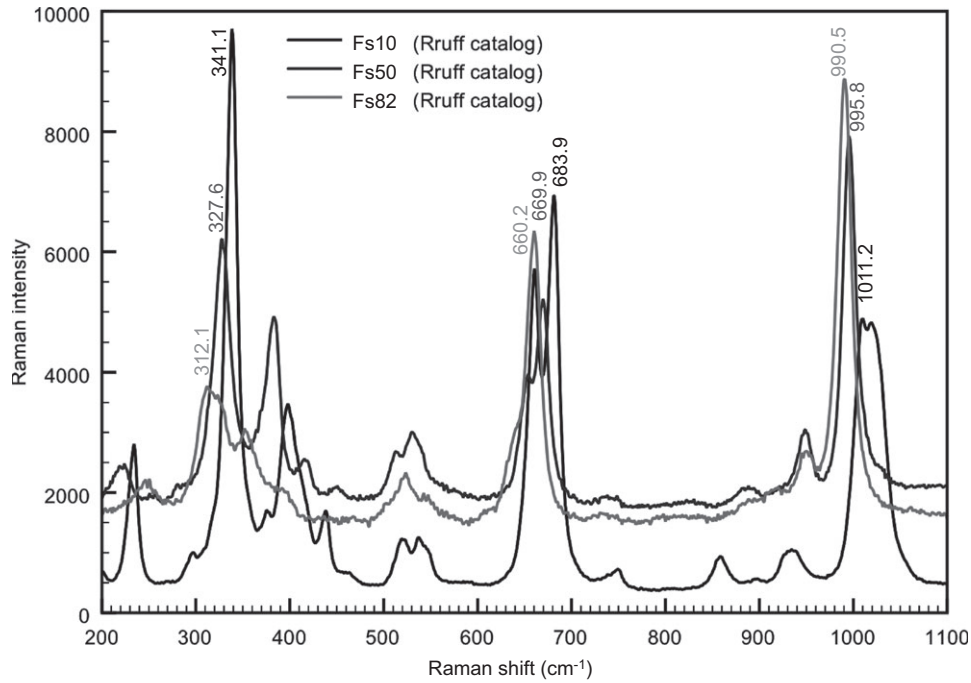

Fig. 6. Raman spectra of reference phases of low-Ca pyroxene. Data from the online database RRUFF. The sample with composition Fs_{10} shows a double Peak B. The far right peak has been selected according with the trend shown by the other two peaks.

$$\text{Fs mole\%} = -3.44x_C + 3479 \quad (6)$$

where x_A is the Raman shift corresponding to Peak A, x_B is the Raman shift corresponding to Peak B, and x_C is the Raman shift corresponding to Peak C.

These curves are corrected for the composition range observed in ordinary chondrites, yielding the following equations:

$$\text{Fs mole\%} = -2.66x_A + 918 \quad (7)$$

$$\text{Fs mole\%} = -3.08x_B + 2116 \quad (8)$$

$$\text{Fs mole\%} = -3.43x_C + 3479 \quad (9)$$

These equations were used for estimating the Raman shift expected for H, L, and LL chondrites, according to the Fs values given in Hutchison (2004) and shown in Table 2.

Three characteristic peaks imply three combinations of peak versus peak plot (Fig. 8). The plot of Peak A versus Peak B offers the best correlation between the reference material and the analyzed grains. Nevertheless, data for enstatite endmembers (theoretical composition Fs_0) do not define a single point but rather exhibit different Raman shifts (Figs. 7a–c and 8; Table 1), reflecting the crystallography: the orthorhombic variety has higher shift than the monoclinic variety (e.g., Ulmer and Stalder 2001). According to this observation, all the analyzed grains in the enstatite chondrite (sample Sahara 97079) likely correspond to the monoclinic variety. Although interesting for the characterization of the samples, this feature increases the error in the calibration curve. The uncertainty in the detection of Peak C affects the plots Peak A versus Peak C (Fig. 8b) and Peak B versus Peak C (Fig. 8c). In detail, the measured values for chondrites do not follow on the linear correlation determined from the reference phases (Figs. 8d–f).

Blind Tests on Randomly Selected Ordinary Chondrites

Six samples from the Antarctic collection, already classified at the NIPR with the aid of microprobe and optical microscopy (Yamaguchi et al. 2014), were tested for chemical group identification by Raman spectroscopy, together with two samples from the Northwestern Africa (NWA) collection at the RBINS (Table 3). Polished chips (PS) in Al-ring and polished thin sections (PTS) were analyzed. Results are shown in Fig. 9. Despite the relatively large error bars (standard deviation corresponding to maximum 0.9 cm^{-1} for Peak A in A 09515, due to the range of Fa content), the identification of the chemical group based on olivine is

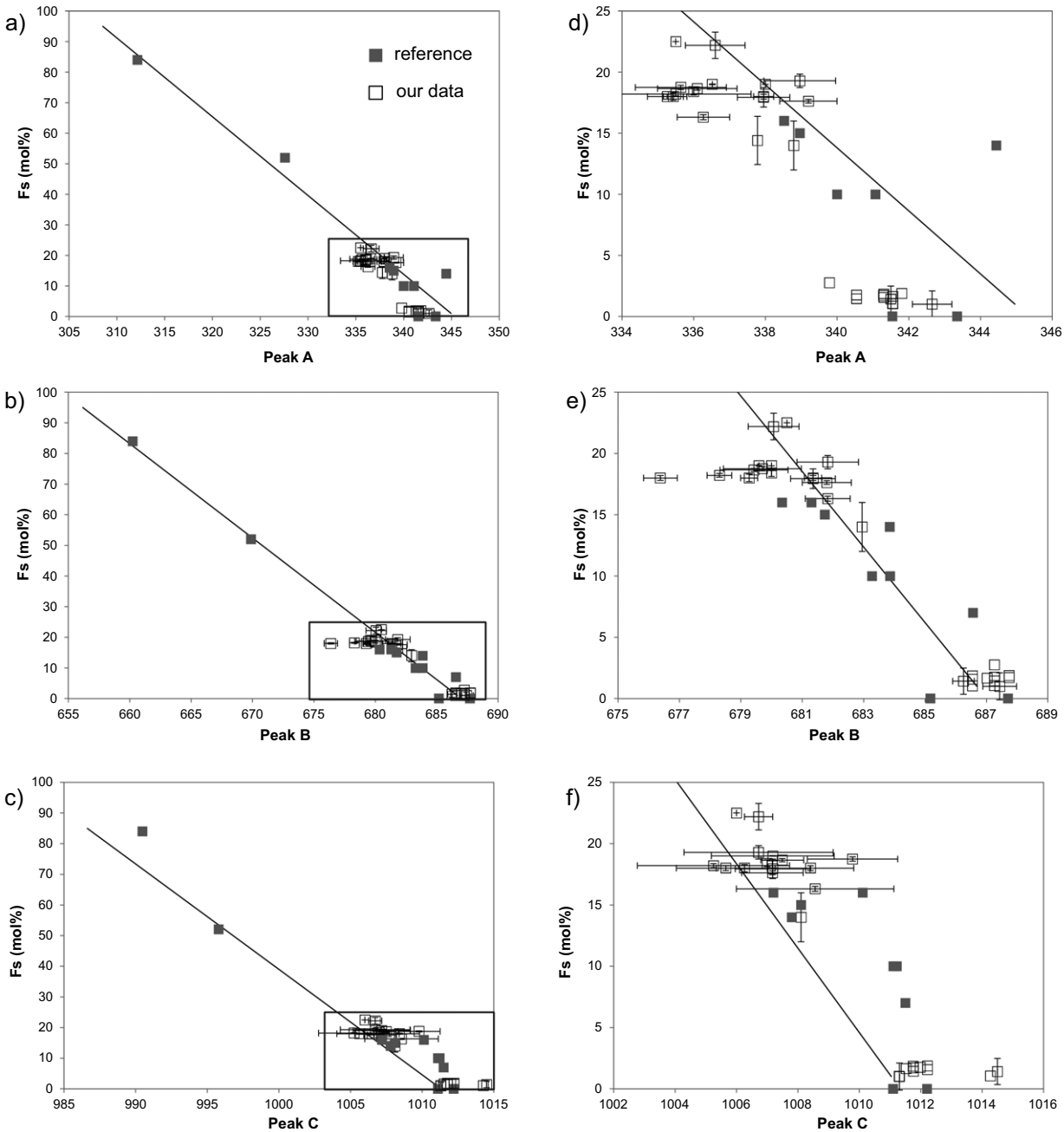

Fig. 7. Correlation between the Fs content in pyroxene and the Raman shift of three selected peaks (Peak A in (a) and Peak B in (b), and Peak C in (c), respectively). A detail view on the analyzed compositional range for the three selected peaks is shown in (d), (e), and (f), respectively.

consistent with the official classification (Fig. 9a and Table 3). Results for pyroxene are less straightforward (Figs. 9b–d), even for highly equilibrated (petrologic type 5–6) samples, especially for A 09515, which has unexpectedly large error bars. Peak A seems the most sensitive to subtle crystallographic or chemical variations. Although highly shocked, sample A 09584 shows good agreement with the chemical group determined by Peak A versus Peak B and Peak B versus Peak C plots (Figs. 9b and 9d). Samples belonging to H do not show any uncertainty in the Raman identification for the chemical group. Overall, Fig. 9 shows that the average information from pyroxene is in agreement with the classification provided by olivine.

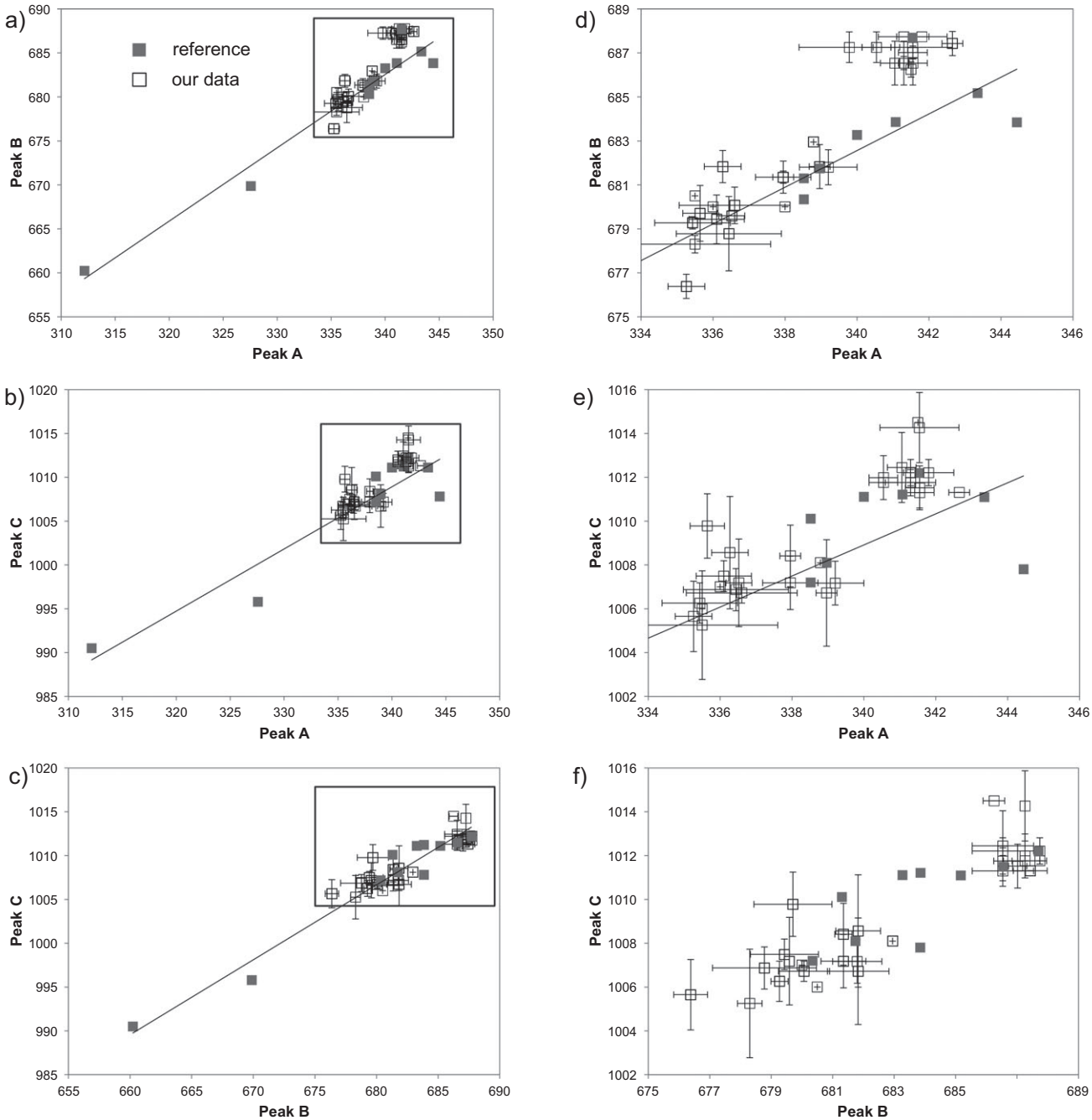

Fig. 8. Peak versus peak plots for pyroxene, Peak A versus Peak B in (a), Peak A versus Peak C in (b), and Peak B versus Peak C in (c). A detail view for the three selected peaks in the measured samples is shown in (d), (e), and (f), respectively.

DISCUSSION

Calibration for Olivine

The peak position versus composition plot shows a good correlation for the samples used as reference. However, the analyzed grains from chondrites do not fit perfectly with the correlation curve for Peak B, although the error bars remain small. The correlation curve obtained from the reference olivines is consistent with data in the literature (e.g., fig. 8a in Wang et al. [2004] and fig. 8 in Kuebler et al. [2006]), therefore the

Table 3. Characteristics of the samples used for blind tests.

Name	Chemical group	Petrologic type	Shock stage[a]	Weathering	PTS/PS	Raman classification
A 09244	L	6	–	B[b]	PS	Good
A 09436	H	3	–	C[b]	PS	Good
A 09515	L	6	–	A/B[b]	PS	Good for Ol, 2/3 for Px
A 09546	L	6	–	C[b]	PS	Good for Ol
A 09584	H	5	S5–6	A/B[b]	PTS	Only Px, 2/3
A 09618	H	5	–	C[2]	PS	Good
NWA 1717	LL	5–6	S4	W1[c]	PTS	Good for Ol within error for Px
NWA 6752	H	3	S1	W2[c]	PTS	Good

[a]According to Stoeffler et al. (1991).
[b]Weathering classification for Antarctic meteorites, according to ANSMET and NIPR.
[c]Weathering classification according to Wlotzka (1993).

cause of the small shift observed in our samples should be found in the measurements. The shift shown for Peak B by some olivine grains in ordinary chondrites might be caused by the presence of secondary elements in the crystal structure, such as a low amount of Mn, or by analytical artifacts. Unfortunately, those measurements could not be checked a second time. It should be noted that on the day of measurements a temporary problem with the calibration might have affected a portion of the spectrum. Nevertheless, this problem almost disappears in the peak versus peak plot and is consistent with a polynomial correlation curve, as observed in the literature (e.g., Kuebler et al. 2006). The possible Mn content in the selected olivine grains was not quantified because no mineral standard for this element was included among those used for the EDX analyses. However, the results suggest that <0.4 wt% possibly consists of elements other than Si, Mg, and Fe and the EDX spectra did not exhibit notable peaks for Mn. Therefore, the bad fitting for Peak B is very likely due to technical problems of the Raman instrument on the day of the analyses. To avoid similar experiences, we recommend to check the calibration of the Raman spectrometer with reference silicon wafer before and after the measurements and to check a "reference" olivine sample, of known composition, every time the classification appears dubious or problematic. Nevertheless, the corrected calibration for olivine in chondritic range (equations 1 and 3) allows correct identification of the chemical group for olivine analyses in blind tests (Fig. 9).

A major concern about the reliability of the correlation curve is the possible presence of ringwoodite, a high-pressure polymorph of olivine with cubic crystal symmetry. Ringwoodite has a Raman spectrum that is quite similar to that of olivine, but with a lower shift of the two characteristic peaks (e.g., Miyamoto and Ohsumi 1995; Gillet et al. 2007; Walton 2013). An inexperienced operator, not familiar with ringwoodite appearance in transmitted light microscopy or not aware of the occurrence of possible shock veins in the sample, might mistakenly use Raman spectra of ringwoodite for those of olivine. The spectrum of ringwoodite is also correlated to the composition (e.g., Feng et al. 2011), but a different calibration is required. For this reason, we recommend avoiding ringwoodite for a fast classification purpose. However, ringwoodite is generally localized along shock veins, which can be easily identified with the optical microscope. Although negligible in meteorites, the grain size difference between samples might also affect the Raman spectrum (Foucher et al. 2012). Thus, an accurate selection of grains to be investigated using the Raman approach, selecting coarse grained crystals, apparently equilibrated, is important for the reliability of the chemical classification of the sample.

Calibration for Low-Ca Pyroxene

Ordinary chondrites might contain minor amounts of Ca-bearing pyroxene. Only based on Raman spectrum, it is difficult to distinguish low-Ca pyroxene from pyroxenes containing >3% Ca. The spectra have similar shape, with three more evident peaks. There is only a slight shift to lower values for peak positions in the case of Ca pyroxene with respect to the low-Ca pyroxene (e.g., Wang et al. 2001). Therefore, good statistics (number of grains analyzed) are important to document the general trend of peak positions within a chondrule, to exclude out-of-trend analyses that might refer to Ca-bearing pyroxene.

In some cases, even the MATLAB/Octave *peakdet* script encountered problems in identifying the characteristic peaks because of a peak duplication effect. The crystallographic orientation of the analyzed pyroxene can affect the Raman spectrum (e.g., Huang et al. 2000). This might result in the duplication of a peak, in certain cases with higher Raman intensity for the secondary peak than for the characteristic peak that is correlated with the chemical composition. Duplication

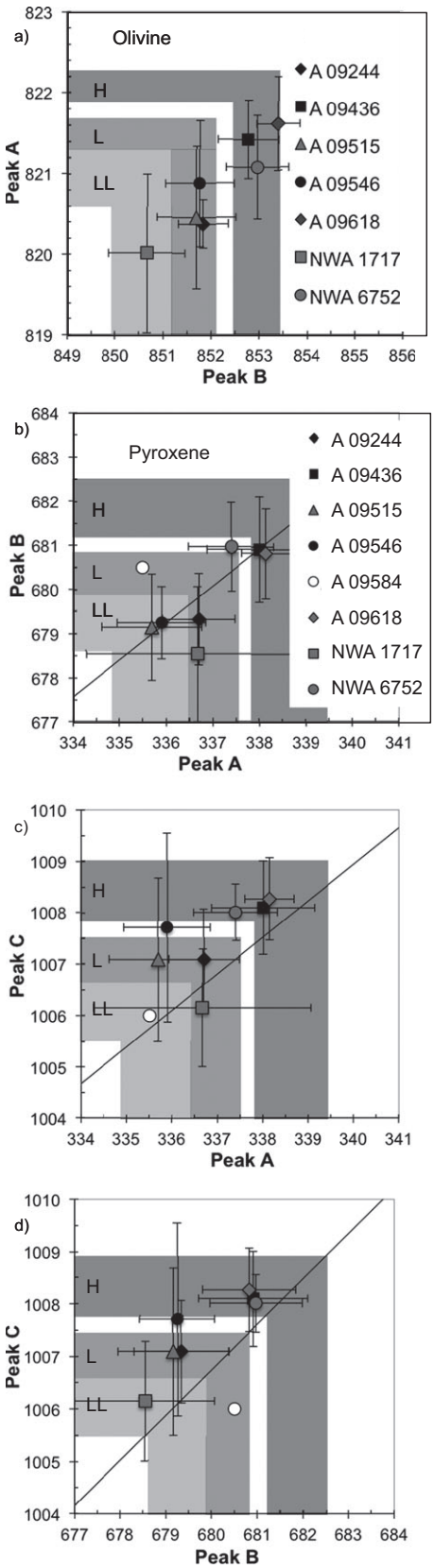

Fig. 9. Chemical group identification by Raman spectroscopy for eight ordinary chondrites. The shaded areas represent the expected range of Raman shift corresponding to H, L, and LL chemical groups, as determined from equations in the text. Each point represents the average value over 30–50 analyses in the sample and the error bars correspond to the standard deviation. Sample A 09584 was measured at NIPR before the development of this technique and, although a limited number of grains could be measured and only of pyroxene, the chemical group identification is consistent with that determined with the microprobe.

and shift of peaks might be induced also by the occurrence of fine-grained exsolution (Wang et al. 2001). However, this duplication effect is never observed simultaneously on all the three characteristic peaks. As the stage used for Raman cannot be tilted during the analyses to find the best orientation for the considered grain, we suggest carefully checking the position of the three characteristic peaks, to predict the expected shift range for the dubious peak compared to the known position of the other two (e.g., the spectrum of Fs_{10} in Fig. 6).

For Peak A, the experimental data from meteorites fit well with the best-fit curve obtained for the reference material. For Peak B and Peak C, the small range of composition investigated constitutes a problem. It might be difficult to select the right peak because peak C, and sometimes also peak B, show the duplication above mentioned.

Raman spectroscopy allows the identification of low-Ca monoclinic pyroxene and the orthorhombic variety (Table 1) (e.g., Ulmer and Stalder 2001). This feature is more an issue for Raman analyses than an advantage, but it occurs only for enstatitic endmembers, which are generally rare in ordinary chondrites.

Chemical Group Identification

According to Van Schmus and Wood (1967), Weisberg et al. (2003), Kessel et al. (2007) and references therein, the chemical group H, L, and LL are distinguishable based on the Fa content in olivine and the Fs content in the low-Ca pyroxene (Table 2). For olivine, the Raman calibration has given reliable results, especially for the peak versus peak plot. Therefore, following Table 2, the chemical group identification should be accurate enough (Fig. 9). In Lunning et al. (2012), although with a different technique, only olivine is considered for the chemical group determination in ordinary chondrites.

The estimate for low-Ca pyroxene might be used as confirmation, because of the complication related to the crystallographic symmetry that might affect the data

(Figs. 9b–d). None of the peak versus peak plots provides a straightforward correlation, but the combination of all is beneficial, because of the influence of two peaks at the same time. Accordingly, the relation between chemical group and peak position for pyroxene is summarized in Table 2.

The chemical group identification based on Fa content in olivine should be always compared with that based on the Fs content in low-Ca pyroxene, at least for confirmation. In the case of strong inconsistency or if other features in the sample point to a different chemical classification, the use of the microprobe is highly recommended. A meaningful number of analyses are necessary for a reliable result. We recommend at least 30 measurements for olivine and 20 for low-Ca pyroxene. For highly equilibrated meteorites, 20 olivine and 10 pyroxene measurements might be enough, but only when the sample clearly exhibits very low standard deviation between measurements and if optical observations also point toward a high petrologic type. Whenever the determined range of data is too large for a clear classification and the optical observations suggest a type 3 chondrite, other techniques might be necessary for the chemical group identification (e.g., Scott and Krot 2005).

Practical Advantages of Using Raman Spectroscopy

The analyses reported here have been performed using both polished thin sections and polished rock chips. The use of a perfectly flat surface allows avoiding the possible contamination of the signal from neighbor phases. However, in comparison with other types of analyses, Raman is less affected by the sample topography. Whenever more than one phase contributes to the Raman spectrum and the characteristic peaks of all phases are distinguishable, the influence from other grains can be immediately recognized and the analysis repeated, adjusting the focus on the selected grain. With the microprobe, for instance, mixed signals can hardly be distinguished, resulting in a composition that is intermediate between the different phases hit by the electron beam. Thus, although not tried for this work, raw samples can potentially be used. Obviously the inner part of the meteorite must be exposed, even better if on a roughly polished surface.

The time for the acquisition of a Raman spectrum is quite short: 20–30 s, depending on the accuracy of the measurement. Analyses are performed in air. High vacuum is not required and the possible problem related to degassing of old epoxy is completely excluded. High-quality reference material, measured under the same conditions as the unknown samples, is not necessary for Raman spectroscopy, although a quick check of the instrument calibration with a silicon wafer is recommended at the beginning and at the end of the analytical session.

As petrographic thin- or polished sections are commonly prepared any way from meteorites for the petrologic type identification (e.g., Weisberg et al. 2003; Lunning et al. 2012), whenever available they can be used for Raman analyses, with no carbon coating that could impair future analyses. The petrologic type can be determined in polished preparations by the shape and distribution of metals (Huss et al. 2006; Devouard and Zanda 2013), preventing the need of a petrographic thin section, which is generally more expensive and difficult to prepare. In addition, Raman spectrometers are generally equipped with an optical, reflected light, microscope. The chemical group and the petrologic type can be, therefore, determined in most samples in one analytical step, only requiring a polished surface. Finally, as the cost of a Raman spectrometer can be relatively low in comparison with fully equipped electron microscope and microprobe, this instrument might be available in institutes that cannot afford large investments.

CONCLUSIONS

The use of Raman spectroscopy is a promising alternative method for the screening and rough chemical classification of large collections of ordinary chondrites. This technique is based on the existing correlation between the Raman shift of selected peaks of olivine and pyroxene and the corresponding Fa and Fs content, respectively. These correlations are not new in the literature, but were never used for a large-scale classification of ordinary chondrites. The advantages of the use of Raman spectroscopy are (1) reduced sample preparation is required (no carbon coating, no extra-fine polishing, no mineral separation). Although not tested for this work the technique should be applicable also on a fresh cut, roughly flat surface. (2) The instrumental calibration, limited to routine check with silicon wafer, does not depend on the type of sample analyzed and no specific reference materials are required. (3) The petrologic type can be determined in the same session if the Raman spectrometer is mounted on a petrographic microscope. (4) No high vacuum is necessary, reducing the possible issues induced by the presence of wet samples or of certain types of epoxy. Although possible causes of error are associated with the presence of shocked phases and to the complexity of the pyroxene spectrum (e.g., in the case of Ca-bearing pyroxenes and duplication of peaks due to the crystallographic orientation), the technique has proven to be reliable in blind tests. A statistically meaningful number of

analyses (30–50 in total, depending on the observed range in peak positions, between olivine and pyroxene) on different grains in the same sample and the comparison between the classification for olivine and for pyroxene separately can dramatically reduce the possibilities of mistaken chemical group evaluation. Although the use of the microprobe is still recommended for problematic samples and for accurate measurements of mineral chemistry, most of the numerous equilibrated ordinary chondrite samples filling the collections could be classified or checked by Raman spectroscopy.

Acknowledgments—The authors thank the National Institute of Polar Research in Tokyo (Japan) and the Royal Belgian Institute of Natural Sciences for the loan of polished thin sections and polished chips of the investigated samples. Christian Burlet of the RBINS is thanked for Raman assistance. Giordano Teza (University of Padova) and David De Vleeschouwer (VUB) are thanked for helpful MATLAB hints and tricks. C. Corrigan and an anonymous reviewer are thanked for the helpful comments. A. Yamaguchi is thanked for the editorial handling and insightful discussions. This work has been founded by the BELAM, SAMBA, and IUAP "Planet Topers" projects, supported by Belgian Science Policy Office (BELSPO). PC also thanks the support of Research Foundation Flanders (FWO), and VD the support of the FRS-FNRS and the ERC StG "ISoSyc".

Editorial Handling—Dr. Akira Yamaguchi

REFERENCES

Bilauer E. 2012. Peakdet MATLAB function description and download page. http://www.billauer.co.il/peakdet.html. Accessed March 18, 2014.

Bonal L., Quirico E., Bourot-Denise M., and Montagnac G. 2006. Determination of the petrologic type of CV3 chondrites by Raman spectroscopy of included organic matter. *Geochimica et Cosmochimica Acta* 70:1849–1863.

Bonal L., Quirico E., Flandinet L., Beck P., and Montagnac G. 2014. Thermal history of primitive chondrites: Short vs. long duration (abstract #5145). 77th Annual Meteoritical Society Meeting. *Meteoritics & Planetary Science* 49.

Devouard B. and Zanda B. 2013. Les transformations sur les corps parents des chondrites. In *Le Règne Minéral, Cahier no. 3, Les météorites primitives*. Glavenas, Saint-Julien-du-Pinet, France: Les Editions du Piat. 98 p (in French).

Downs R. T. 2006. The RRUFF Project: an integrated study of the chemistry, crystallography, Raman and infrared spectroscopy of minerals. Program and Abstracts of the 19th General Meeting of the International Mineralogical Association in Kobe, Japan. O03-13.

Feng L., Lin Y., Hu S., Xu L., and Miao B. 2011. Estimating compositions of natural ringwoodite in the heavily shocked Grove Mountains 052049 meteorite from Raman spectra. *American Mineralogist* 96:1480–1489.

Foucher F., Lopez-Reyes G., Bost N., Rull-Perez F., Rüßmann P., and Westall F. 2012. Effect of grain size distribution on Raman analyses and the consequences for *in situ* planetary missions. *Journal of Raman Spectroscopy* 44:916–925.

Gillet P., El Goresy A., Beck P., and Chen M. 2007. High-pressure mineral assemblages in shocked meteorites and shocked terrestrial rocks: Mechanisms of phase transformations and constraints to pressure and temperature histories. *GSA Special Papers* 421:57–82.

Haskin L. A., Wang A., Rockow K. M., Jolliff B. L., Korotev R. L., and Viskupic K. M. 1997. Raman spectroscopy for mineral identification and quantification for in situ planetary surface analysis: A point count method. *Journal of Geophysical Research* 102:19,293–19,306.

Huang E., Chen C. H., Huang T., Lin E. H., and Xu J. 2000. Raman spectroscopic characteristics of Mg-Fe-Ca pyroxenes. *American Mineralogist* 85:473–479.

Huss G. R., Rubin A. E., and Grossman J. N. 2006. Thermal metamorphism in chondrites. In *Meteorites and the early solar system II*, edited by Lauretta D. S. and McSween H. Y. Jr. Tucson, Arizona: The University of Arizona Press. pp. 567–586.

Hutchison R. 2004. *Meteorites: A petrologic, chemical and isotopic synthesis*. Cambridge, UK: Cambridge University Press. 506 p.

Idomar Y., Chennaoui Aoudjehane H., Jambon A., Elkerni H., Larouci N., and Mongy Young P. 2014. Statistical considerations on meteorites from Morocco and Northwest Africa (NWA) (abstract #5351). 77th Annual Meteoritical Society Meeting. Meteoritics & Planetary Science 49.

Jarosewich E. 1990. Chemical analyses of meteorites: A compilation of stony and iron meteorite analyses. *Meteoritics* 25:323–337.

Kallemeyn G. W., Rubin A. E., Wang D., and Wasson J. T. 1989. Ordinary chondrites: Bulk compositions, classification, lithophile-element fractionations, and composition-petrographic type relationships. *Geochimica et Cosmochimica Acta* 53:2747–2767.

Kessel R., Becktee J. R., and Stolper E. M. 2007. The thermal history of equilibrated ordinary chondrites and the relationship between textural maturity and temperature. *Geochimica et Cosmochimica Acta* 71:1855–1881.

Krot A. N., Keil K., Goodrich C. A., Scott E. R. D., and Weisberg M. K. 2005. Classification of meteorites. In *Meteorites, comets and planets*, edited by Davis A. M. Treatise on Geochemistry, vol. 1. Amsterdam, the Netherlands: Elsevier B.V. pp. 83–128.

Kuebler K. E., Jolliff B. L., Wang A., and Haskin L. A. 2006. Extracting olivine (Fo–Fa) compositions from Raman spectral peak positions. *Geochimica et Cosmochimica Acta* 70:6201–6222.

Lunning G., Corrigan C., Welzenbach L. C., and McCoy T. J. 2012. Using immersion oils to classify equilibrated ordinary chondrites from Antarctica (abstract #1566). 43rd Lunar and Planetary Science Conference. CD-ROM.

Miyamoto M. and Ohsumi K. 1995. Micro Raman spectroscopy of olivines in L6 chondrites: Evaluation of the degree of shock. *Geophysical Research Letters* 22:437–440.

Quirico E., Montagnac G., Rouzaud J.-N., Bonal L., Bourot-Denise M., Duber S., and Reynard B. 2009. Precursor and metamorphic condition effects on Raman spectra of

poorly ordered carbonaceous matter in chondrites and coals. *Earth and Planetary Science Letters* 287:185–193.

Rochette P., Sagnotti L., Bourot-Denise M., Consolmagno G., Folco L., Gattacceca J., Osete M. L., and Pesonen L. 2003. Magnetic classification of stony meteorites: 1. Ordinary chondrites. *Meteoritics & Planetary Science* 38:251–268.

Rubin A. E. 1990. Kamacite and olivine in ordinary chondrites: Intergroup and intragroup relationships. *Geochimica et Cosmochimica Acta* 54:1217–1232.

Scott E. R. D. and Krot A. N. 2005. Chondritic meteorites and the high-temperature nebular origins of their components. In *Chondrites and the protoplanetary disk*, edited by Krot A. N., Scott E. R. D., and Reipurth B. *ASP Conference Series* 341:15–54.

Stoeffler D., Keil K., and Scott E. R. 1991. Shock metamorphism of ordinary chondrites. *Geochimica et Cosmochimica Acta* 55:3845–3867.

Ulmer P. and Stalder R. 2001. The $Mg(Fe)SiO_3$ orthoenstatite-clinoenstatite transitions at high pressures and temperatures determined by Raman-spectroscopy on quenched samples. *American Mineralogist* 86:1267–1274.

Van Schmus W. R. and Wood J. A. 1967. A chemical-petrologic classification for the chondritic meteorites. *Geochmica et Cosmochimica Acta* 31:747–765.

Walton E. L. 2013. Shock metamorphism of Elephant Moraine A79001: Implications for olivine–ringwoodite transformation and the complex thermal history of heavily shocked Martian meteorites. *Geochimica et Cosmochimica Acta* 107:299–315.

Wang D. and Chen M. 2006. Shock-induced melting, recrystallization, and exsolution in plagioclase from the Martian lherzolitic shergottite GRV 99027. *Meteoritics & Planetary Science* 41:519–527.

Wang A., Jolliff B. L., Haskin L. A., Kuebler K. E., and Viskupic K. M. 2001. Characterization and comparison of structural and compositional features of planetary quadrilateral pyroxenes by Raman spectroscopy. *American Mineralogist* 86:790–806.

Wang A., Kuebler K., Jolliff B., and Haskin L. A. 2004. Mineralogy of a Martian meteorite as determined by Raman spectroscopy. *Journal of Raman Spectroscopy* 35:504–514.

Wasson J. T. and Kallemeyn G. W. 1988. Composition of chondrites. *Philosophical Transactions of the Royal Society of London A* 325:535–544.

Weisberg M. K., McCoy T. J. M, and Krot A. N. 2003. Systematics and evaluation of meteorite classification. In *Meteorites and the early solar system II*, edited by Lauretta D. S. and McSween H. Y. Jr. Tucson, Arizona: The University of Arizona Press. pp. 19–52.

Wlotzka F. 1993. A weathering scale for the ordinary chondrites (abstract). *Meteoritics* 28:460.

Wolverson D. 1995. Raman spectroscopy. In *An introduction to laser spectroscopy*, edited by Andrews D. L. and Demidov A. A. New York: Springer. pp. 91–114.

Yamaguchi A., Pittarello L., Kimura M., and Kojima H. 2014. Meteorite Newsletter 23. Tokyo: NIPR.